Journal of The Electrochemical Society, **157** (5) H551-H556 (2010)
0013-4651/2010/157(5)/H551/6/$28.00 © The Electrochemical Society

Growth and Interface Evolution of HfO_2 Films on GaAs(100) Surfaces

Theodosia Gougousi,[a,z] Justin C. Hackley,[a,*] J. Derek Demaree,[b] and John W. Lacis[a]

[a]*Department of Physics, University of Maryland Baltimore County, Baltimore, Maryland 21250, USA*
[b]*Weapons and Materials Research Directorate, Army Research Laboratory, Maryland 21005-5069, USA*

The initial film growth (2–100 cycles) and the interface evolution of HfO_2 thin films on GaAs surfaces were investigated for an atomic layer deposition chemistry that utilizes tetrakis(ethylmethyl) amino hafnium and H_2O at 250°C. Starting surfaces include native oxide and HF or NH_4OH-etched substrates. X-ray photoelectron spectroscopy shows that deposition on native oxide GaAs surfaces results in the gradual consumption of the arsenic and gallium oxides. Arsenic oxides are easier to remove, leaving some metallic arsenic–arsenic suboxide at the interface. The removal of the gallium oxides is slower, and some residual Ga_2O_3 and Ga_2O are detected after 100 process cycles. High resolution transmission electron microscopy confirms the presence of an almost sharp interface for the 100 cycle (12 nm) film and indicates that the as-deposited film is polycrystalline. The depositions on either HF or NH_4OH-etched substrates result in a sharp interface with very little residual gallium oxide and arsenic suboxide present. Rutherford backscattering spectroscopy shows that steady-state growth comparable to that achieved on SiO_2 is reached after ~20 ALD cycles for all GaAs surfaces; however, high initial surface activity is detected for the etched surfaces.
 [DOI: 10.1149/1.3353166]

Manuscript submitted December 1, 2009; revised manuscript received January 12, 2010. Published April 6, 2010.

The deposition of high dielectric constant (high-*k*) materials has been studied extensively in the past decade as a potential replacement to SiO_2 in an effort to extend the lifetime of Si-based nanoelectronic devices. One of the major obstacles encountered in the introduction of high-*k* materials has been the inadvertent growth of low dielectric constant interfacial layers (ILs).[1] Although the presence of ILs improves the interface properties of the gate stack, it also results in the overall reduction in the stack capacitance, negating much of the benefit afforded by the introduction of the high-*k* material.[2] Alternative, higher mobility substrates such as Ge and III-V-based semiconductors are well known, but their use in the microelectronics industry has been hampered by the absence of a high quality native oxide comparable to the Si/SiO_2 system.[3] However, extensive research into high-*k* materials has led to a renewed interest in the pairing of high mobility substrates with high-*k* materials in future generations of nanoelectronic devices. Although the deposition of dielectrics on Si surfaces is invariably accompanied by the formation of an IL regardless of the deposition technique, several reports demonstrate a sharp interface between the high-*k* and the high mobility substrate. In fact, several groups have demonstrated well-behaved devices utilizing Al_2O_3 and HfO_2 dielectrics on Ge-, GaAs-, and InGaAs-based substrates.[4-8] When atomic layer deposition (ALD) is used for the deposition of Al_2O_3, TiO_2, and HfO_2 dielectrics on GaAs and InGaAs native oxide surfaces, the thinning of these surface oxides is observed. All these observations share the common thread of the use of metallorganic precursors such as trimethyl aluminum and hafnium and titanium amides.[9-18]

In this work, we utilize ALD to deposit HfO_2 films on both native oxide and etched GaAs surfaces. The Hf precursor chosen is tetrakis(ethylmethyl) amino hafnium (TEMAHf), and H_2O is used as the oxidizer. We primarily use X-ray photoelectron spectroscopy (XPS) to study the evolution of the interface as a function of the process cycle number, and for depositions on native oxide surfaces, we demonstrate the existence of a gallium and arsenic oxide consumption mechanism during the deposition process. These findings are corroborated by high resolution transmission electron microscopy (HRTEM) data. The predeposition treatment of the substrate in either HF or NH_4OH passivates the interface and prevents the reoxidation of the interface. Rutherford backscattering spectroscopy (RBS) is used to characterize the film growth on all starting surfaces.

Experimental

The HfO_2 depositions were performed in a homebuilt ALD reactor.[19] The hot-wall flow-tube reactor was computer-controlled via a Labview routine. The modular metallorganic precursor delivery system was placed in an oven to ensure uniform heating of all surfaces and lines. TEMAHf and H_2O were used as the precursors, and the depositions were performed at 250°C with 30 s purge time between the reagent pulses. Both reagents were delivered using the fixed volume approach described by Hausmann et al.[20] To ensure sufficient vapor pressure, the TEMAHf container was heated to 106°C, and the water vessel was kept at room temperature. Three different GaAs(100) surfaces were examined: (*i*) "Native oxide" surfaces: Pieces of GaAs wafers were cleaned in acetone, methanol, followed by a quick deionized (DI) water rinse and N_2 blow dry. (*ii*) "NH_4OH" surfaces: Wafer pieces were dipped in JT Baker (JTB)-100 clean for 5 min, followed by a DI water rinse, etched in a 30% NH_4OH aqueous solution for 3 min, and finished with a quick DI rinse and N_2 blow dry. (*iii*) "HF" surfaces: Wafer pieces were dipped in JTB for 5 min, followed by a DI water rinse, etched in buffered oxide etch for 20 s, and finished with a quick DI rinse and N_2 blow dry. The HF and NH_4OH samples were loaded into the reactor immediately following the preparation to minimize the surface ambient exposure. Si control samples were prepared by soaking the pieces of native-oxide-covered Si(100) in JTB for 5 min, DI rinsed for 5 min, and N_2 blow dry.

Ex situ XPS was used to examine the composition of the interface and performed with a Kratos AXIS 165 (Al X-ray source, 1486.6 eV), equipped with a hemispherical analyzer (165 mm radius). High resolution spectra of the As $2p_{3/2}$, As 3d, and Ga $2p_{3/2}$ regions were recorded at a 0.1 eV step size, a 20 eV pass energy, without charge neutralization, and with photoelectron emission normal to the sample surface. With the exception of the 100 cycle film that was sputter-thinned in the analytical chamber to permit recording of the Ga $2p_{3/2}$ and As $2p_{3/2}$ regions that have very small inelastic mean free paths and, as a result, are very surface sensitive, no other samples were sputter-cleaned before the analysis.[21] The high resolution spectra were baseline-corrected and separated into their components using Gaussian–Lorentzian functions. The Lorentzian component was set at 40% for all peaks. In the As 3d region, the substrate As $3d_{5/2}$ and As $3d_{3/2}$ doublet was analyzed by assuming functions of equal full width at half-maximum (fwhm), a spin-orbit

* Present address: Laboratory for Physical Sciences, 8050 Greenmead Drive, College Park, MD 20740.
z E-mail: gougousi@umbc.edu

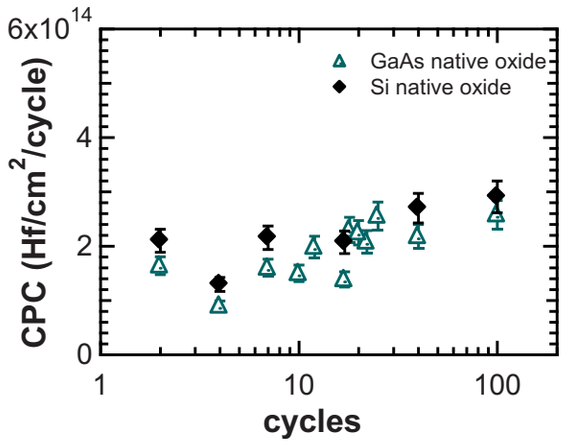

Figure 1. (Color online) Hf atom CPC obtained by RBS for a series of samples deposited on native oxide GaAs and Si native oxide control samples.

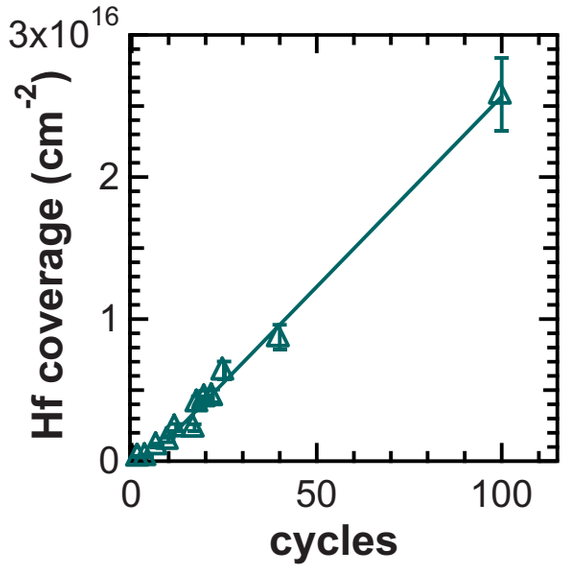

Figure 2. (Color online) Hafnium atom surface coverage measured by RBS for a series of films deposited on GaAs native oxide surfaces. The solid line is the linear regression line for the data obtained for samples thicker than 10 ALD cycles.

separation of 0.7 eV, and an intensity ratio of 3:2, and the substrate As $3d_{5/2}$ peak (As–Ga) was placed at a binding energy of 41.1 eV. The arsenic oxide contribution was estimated using separate peaks for As_2O_3 (44.4 ± 0.1 eV), As_2O_5 (45.6 ± 0.1 eV), and an arsenic suboxide–metallic arsenic component As^0–AsO_x (42.1 ± 0.1 eV).[22,23] The As $2p_{3/2}$ region was similarly analyzed using a peak for each of the three oxidation states described before (As^0–AsO_x: 1324.3 ± 0.3 eV, As_2O_3:1326.3 ± 0.1 eV, As_2O_5: 1327.7 ± 0.1 eV) in addition to the substrate peak (1323.1 ± 0.1 eV).[13,24] This peak assignment produced a consistent native oxide distribution between the As 3d and As $2p_{3/2}$ areas. In the Ga $2p_{3/2}$ region, the spectra were fitted with peaks for Ga_2O at 1118.3 ± 0.1 and Ga_2O_3 (1119.1 ± 0.1 eV) components in addition to the substrate peak (1117.3 ± 0.1 eV).[22,24] The charge compensation was performed using the binding energies for the As 3d and As $2p_{3/2}$ substrate peaks. Bright field transmission electron microscopy (TEM) and HRTEM data were provided by the TEM Analysis Services Laboratory. The samples were prepared by conventional TEM sample preparation methods using Ar ion beam milling. Bright field images were imaged on a Philips 420 TEM at 120 KV, and HRTEM images were performed on an FEI Tecnai at 200 KV.

Rutherford backscattering spectrometry measurements were made using a 1.2 MeV He^+ beam obtained from a National Electrostatics 5SDH-2 positive ion accelerator. The backscattering angle was 170°, and the spectra were collected using a surface barrier detector subtending approximately 5 msr. The raw RBS data were fitted using the simulation program RUMP.[25] To afford a fair comparison and to prevent process variations from interfering with the study conclusions, all the depositions on the GaAs-etched surfaces as well as the GaAs native oxide and Si control samples (Fig. 1) were performed simultaneously. Additionally, a small sample size (<1 cm^2) was chosen, and the three starting surfaces were placed within a 4 cm^2 area on the sample holder. Earlier depositions on Si surfaces have shown that the film growth variation was insignificant for this sample placement.

Results

Deposition on native oxide surfaces.— A series of thin films from 2 to 100 ALD cycles was deposited on native oxide GaAs surfaces. The hafnium atom surface coverage was measured with RBS, and the data are presented in Fig. 2. The growth appears somewhat retarded initially, but a linear growth is established after approximately 20 process cycles. A subset of these samples was used for the interface evolution study, and Fig. 3 displays high resolution scans of the As 3d and Ga $2p_{3/2}$ regions for the starting native oxide surface and 18-, 20-, 25-, and 100 cycle HfO_2 films. The 100 cycle film was sputter-thinned in the XPS chamber. For each region, we chose to normalize the spectra to the corresponding substrate peak and overlay the spectra to show the difference in the peak shape and width as a function of the ALD process cycle number. For the As 3d region, the change is obvious as the As–O peak is separated clearly from the substrate As peak, and a gradual reduction in the As–O intensity is observed as the film thickness increases. Although the absolute intensity of the As–O peak is reduced as the HfO_2 film grows, the ratio of the As–O to the As substrate peak (As–Ga) is immune to this complication due to the exponential attenuation of the photoelectron intensity. For a stable As–O layer, the ratio of the As–O to the As–Ga peak should be constant and independent of the thickness of the HfO_2 overlayer. If the As–O is consumed, then this translates to a reduction in the ratio of the As–O to the As–Ga peak area, which is exactly what Fig. 3a shows. The film growth can be monitored by the appearance of the shoulder at ~39 eV, which is due to the Hf $5p_{1/2}$ peak from HfO_2 that partially overlaps the As 3d region.

The overlap of the gallium oxide and gallium substrate peaks in the Ga $2p_{3/2}$ region complicates the analysis of the data. However,

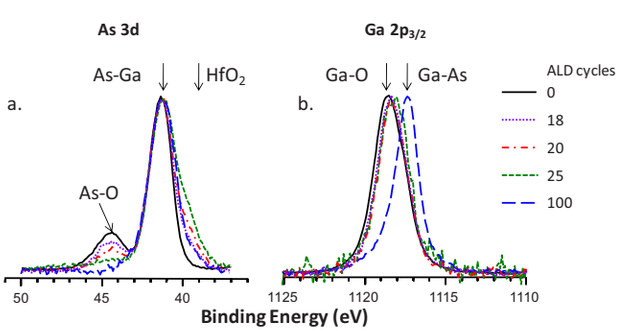

Figure 3. (Color online) (a) As 3d and (b) Ga $2p_{3/2}$ high resolution XP spectra for a series of samples deposited on native oxide GaAs surface. The spectra have been overlaid to illustrate the gradual thinning of the interfacial arsenic and gallium native oxides.

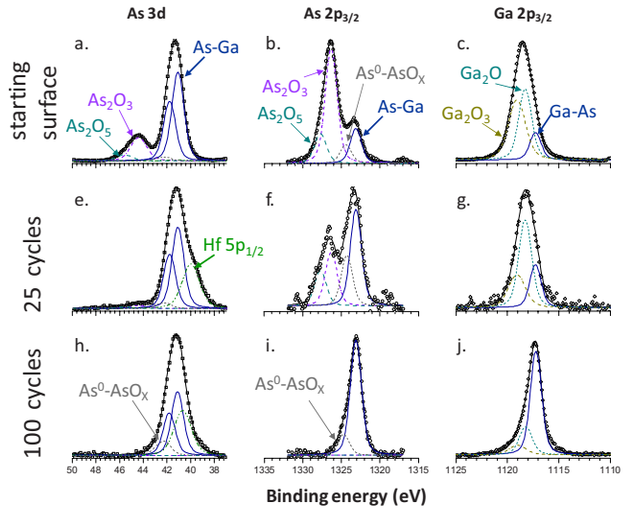

Figure 4. (Color online) [(a)–(c)] As 3d, As $2p_{3/2}$, and Ga $2p_{3/2}$ high resolution XP spectra for the starting surface, [(e)–(g)] a 25 cycle film, and [(h)–(j)] a 100 cycle film deposited on native oxide GaAs surface. After 100 ALD cycles, most of the starting surface native oxides have been consumed and some As^0–AsO_x has accumulated at the interface.

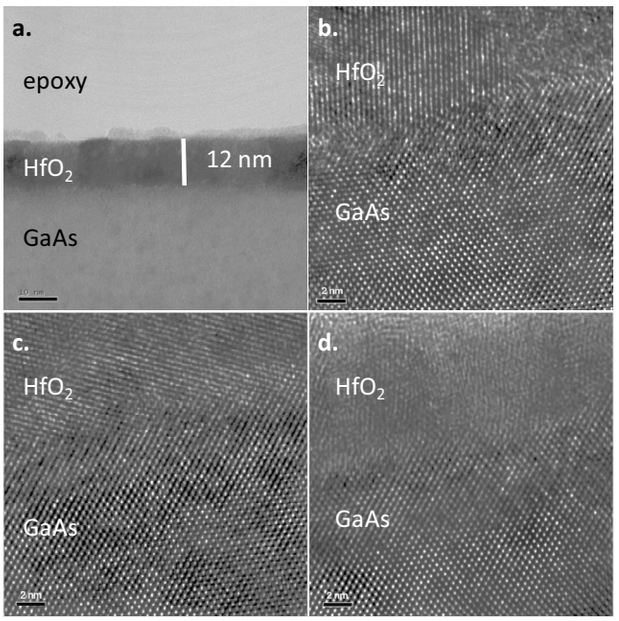

Figure 5. (a) Bright field TEM and [(b)–(d)] HRTEM images for the as-deposited 100 cycle film prepared on native oxide GaAs. A practically sharp interface is obtained between the GaAs substrate and the polycrystalline HfO_2 film.

as shown in Fig. 3b, there is a marginal reduction in the fwhm of the Ga peak between the starting surface and after 18 and 20 ALD cycles. At 25 cycles, the peak shape is more symmetric and is shifted at a lower binding energy. At 100 ALD cycles, the peak fwhm is noticeably smaller and is shifted at an even lower binding energy. All these observations are consistent with a gradual removal of some of the gallium oxides from the interface.

To illustrate better, the native oxide removal during the film growth, the data for the As 3d, Ga $2p_{3/2}$, and, additionally, the As $2p_{3/2}$ regions were deconvolved, as described earlier, and the results for the starting surface, the 25 and 100 cycle films, are presented in Fig. 4. Both the As 3d and As $2p_{3/2}$ data confirm that during the first 25 process cycles, almost all of the As_2O_5 and As_2O_3 are removed from the interface, while some As^0–AsO_x accumulates. At 100 ALD cycles, the only arsenic-containing species at the interface is the metallic arsenic–arsenic suboxide, whose abundance has increased compared to the 25 cycle sample. A similar analysis of the spectra for all samples included in Fig. 3 indicates that the As^{5+} component is the easier one to remove, as evidenced by the loss of the higher binding energy component of the arsenic oxide peak in Fig. 3a.

The removal of the interfacial gallium oxides is not as efficient; after 25 process cycles, about half of the Ga_2O_3 is removed with no significant change in the Ga_2O. After 100 ALD cycles, a substantial difference in the Ga peak shape and width is observed, and the peak deconvolution indicates that only traces of Ga_2O_3 and some Ga_2O are still detected.

To confirm the XPS-based observations, a piece of the same as-deposited 100 cycle film was used to obtain the bright field and HRTEM data, and the results are shown in Fig. 5. Figure 5a shows a bright field image of the film, whose thickness is measured at ~12 nm, which agrees well with the previous growth rate data.[19] The image shows the existence of grains in the film, as evidenced by the dark-light contrast areas. The high resolution data shown in Fig. 5b-d confirm that the HfO_2 film is polycrystalline with a variety of grain orientations. The images also confirm the presence of a sharp, albeit not very smooth, interface between the HfO_2 film and the GaAs substrate, corroborating the XPS results that the initial surface native oxide has almost been completely removed during the film deposition.

The growth of the films on native oxide GaAs surfaces has been monitored using RBS, and the hafnium coverage per cycle (CPC) is presented in Fig. 1 as a function of the number of ALD cycles. On the same plot, we include data for films on native oxide Si control samples that were codeposited with the GaAs native oxide samples. The growth rate on the GaAs native oxide is comparable with that on the Si native oxide and in agreement with earlier results for depositions on Si chemical oxide surfaces.[19] The etching reaction that takes place on the native oxide GaAs surface does not appear to affect the film growth rate significantly.

Deposition on pretreated GaAs surfaces.— In a previous work, we have demonstrated that both the HF- and NH_4OH-based treatments remove most of the GaAs surface native oxides.[15] In Fig. 6, we present the As 3d and Ga $2p_{3/2}$ XP spectra of the interface region for a 20 cycle film deposited on NH_4OH-treated surface and a 30 cycle film deposited on a HF-treated GaAs surface. Both surface treatments show no As_2O_3 or As_2O_5 at the interface and the presence of a significantly lower concentration of As^0–AsO_x compared to films of similar thicknesses deposited on the native oxide surfaces. However, both spectra show the presence of some residual Ga_2O_3 and Ga_2O at the interface. The potential effect of this on the electrical properties of the stack is discussed later.

The growth of the films on the etched starting surfaces was studied using RBS, and the hafnium atom CPC is presented in Fig. 7a as a function of the ALD cycles. The 2 cycle samples on both the HF- and NH_4OH-treated surfaces show a much higher hafnium atom that the average CPC obtained for higher cycle samples on the same surfaces as well as those on the native oxides. For the 4 cycle samples, the surface coverage for the HF and NH_4OH surfaces is consistently higher than that for the native oxide surface, but a process variation resulted in a lower overall HfO_2 coverage, masking this effect. To elucidate this in Fig. 7b, we plot the ratio of the surface coverage measured by RBS for the etched to the native oxide surface for the same cycle samples. This comparison is valid because the depositions on all three GaAs surfaces were performed simultaneously and permits a direct comparison of the surface reactivity without having the added complication of the inevitable process variations. Both etched surfaces exhibit an enhanced hafnium

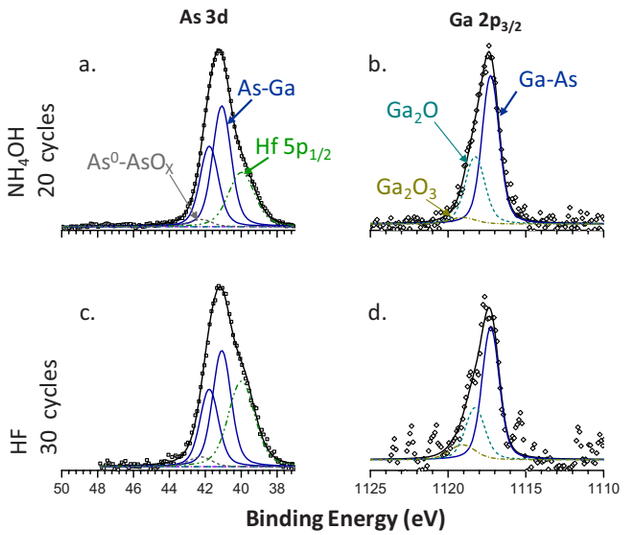

Figure 6. (Color online) [(a) and (b)] As 3d and Ga $2p_{3/2}$ high resolution XP spectra for a 20-cycle film deposited on NH_4OH-etched GaAs and [(c) and (d)] a 30 cycle film deposited on HF-etched GaAs. Very little arsenic and gallium oxide is detected at the interface.

coverage compared to the native oxide initially. As the HfO_2 film grows and covers the initial surface, the growth rate for all three surfaces becomes predictably similar.

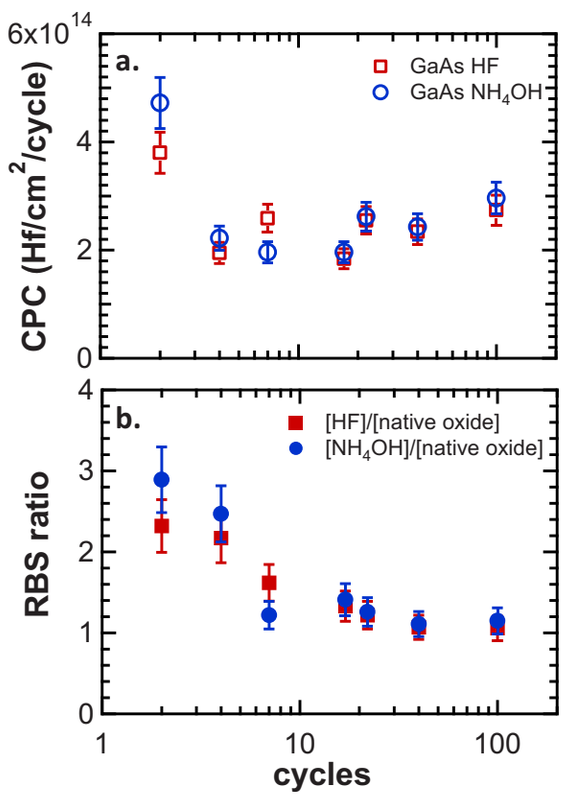

Figure 7. (Color online) (a) Hf atom CPC obtained by RBS for a series of samples deposited on HF- and NH_4OH-etched GaAs surfaces. (b) For the first few ALD cycles, the growth on the etched surfaces is two to three times faster than that obtained on the native oxide GaAs surfaces. After ~10 cycles, the growth on all three GaAs surfaces is very similar.

Discussion

Interface of HfO_2 films on native oxide GaAs surfaces.— When HfO_2 films are deposited on native oxide GaAs surfaces, a gradual thinning of the interfacial oxides is observed. This gradual reduction in the As and Ga oxide intensity can be explained if one assumes that a by-product of the ALD reaction is the active species. Because each ALD cycle deposits a fraction of a HfO_2 monolayer, it produces limited quantities of the by-product that can either volatilize or react with the surface oxides. To remove several monolayers of surface oxides, several ALD cycles are needed, which is indeed what we observed. According to the prevailing mechanism, the most probable reaction by-product for the precursor used in this work would be an ethylmethyl amine molecule produced via hydrogen abstraction by the alkyl amine ligand.[26] Further evidence for this conjecture is provided by the well-established use of the decomposition of organic complexes such as tris(dimethylamino) arsenic and tris(dimethylamino) antimony for the preparation of oxide-free GaAs surfaces at temperatures above 450°C.[27-29] These complexes begin to decompose at temperatures above 300°C, producing dimethylamine and N-methylmethyleneimine that have been shown to etch the GaAs native oxides.[30,31] The ALD reaction examined in this work produces similar amine products through either a regular hydrogen abstraction or β-hydride elimination pathway. At the deposition temperature used (250°C), the precursor is stable, making the ALD reaction the only possible source of these products.

There is evidence that both As_2O_3 and As_2O_5 can react with the GaAs substrate, leading to the formation of Ga_2O_3 and metallic As.[32] The accumulation of As^0–AsO_x that is shown in Fig. 4 may be evidence for the contribution of that mechanism to our observations and corroborates earlier observations for similar ALD chemistries.[13,33] However, although this substrate reaction may contribute to the removal of the As oxides from the interface, it cannot account for the almost-complete removal of both the arsenic and gallium oxides we are observing. If that was the case, then a similar interface cleaning should also have been observed regardless of the ALD chemistry. But, for example, Frank et al. did not observe any interfacial oxide thinning during the ALD of HfO_2 from $HfCl_4$ and H_2O.[10] Furthermore, the concentration of As^0–AsO_x accumulating at the interface is significantly lower than the concentration of the arsenic oxides at the starting surface. Because the desorption of elemental arsenic is low at the deposition temperature of 250°C, most likely, XPS is detecting all of the created As^0–AsO_x.[34] As a result, we conclude that the substrate reaction, while contributing to the interface cleaning, is only a secondary pathway.

For the arsenic oxides, the As^{5+} state appears to be easier to remove than the As^{3+} state, which agrees well with the earlier observation by Hinkle et al.[13] The removal of the higher arsenic oxidation state is thermodynamically unfavorable because the standard heat of formation for As_2O_5 (~91.5 kJ/mol) is higher than that of As_2O_3 (~65.3 kJ/mol).[35,36] Hinkle et al.[13] explained their observations using a charge balance argument, suggesting that it may be energetically favorable for Hf to replace the higher coordinated As^{5+} state rather than the As^{3+} state because Hf atoms prefer the higher coordination configuration. Although this argument offers a plausible explanation for the faster removal of As_2O_5 over As_2O_3, alternative mechanisms may also be present. For example, it has been demonstrated that As_2O_5 can be converted into As_2O_3 and O_2.[35]

Figures 3 and 4 show that the removal of the gallium oxides is slower compared to the arsenic oxides. Similar to the arsenic oxides, the higher gallium oxidation state Ga_2O_3 is easier to remove than Ga_2O, although Ga_2O_3 is more stable thermodynamically (ΔH^0 ~ 1090 kJ/mol for Ga_2O_3 vs ~356 kJ/mol for Ga_2O).[37,38] Although the removal reaction of the gallium oxides may be inherently slower than that for the arsenic oxides, there are also some other contributing factors: (*i*) The analysis of the XPS spectra has shown the starting native oxide to be gallium-rich with a ratio of Ga to As atoms of about 2:1. Such observations agree well with prior observations for thermal GaAs oxides that have been shown to be con-

sistently Ga-rich.[32] (*ii*) The reaction of the arsenic oxides with the substrate may provide an additional source of Ga_2O_3. However, based on the previous discussion, this channel is expected to be of secondary importance.

After 100 ALD cycles, traces of Ga_2O_3 and some Ga_2O are observed at the interface. Although the presence of Ga_2O at the interface has been shown not to cause a Fermi level pinning,[39-41] the presence of even traces of Ga_2O_3 may be problematic due to its adverse effect on the electric properties of the stack.

Interface of HfO_2 films on etched GaAs surfaces.— Very thin films deposited on HF- and NH_4OH-etched GaAs surfaces show less accumulation of As^0–AsO_x and the presence of very little Ga_2O_3 at the interface compared to films of similar thicknesses deposited on native oxide surfaces. These observations may have significant implications about the electrical properties of the stack as the presence of As^0 has been linked to large hysteresis and frequency dispersion in accumulation[33] and that of Ga_2O_3 to the Fermi level pinning.[39-41]

Growth of HfO_2 films on native oxide GaAs surfaces.— When the native oxide GaAs is used as a starting surface, growth is slow for the initial ~15 to 20 cycles but approaches steady-state linear growth after that. Growth is very similar for the Si native oxide control samples that were codeposited with the GaAs samples and comparable to the growth rate measured on Si chemical oxide surfaces.[19] These observations illustrate the fact that once a monolayer coverage of the substrate is accomplished, the starting surface does not affect the bulk film growth.

HRTEM data indicate that the 100 cycle as-deposited films are polycrystalline with the grain size approximately equal to the film thickness. This result is rather unexpected as the previous analysis of similar HfO_2 films deposited on both native oxide and H-terminated Si surfaces have been shown to be amorphous.[42] However, the lattice constant for GaAs (5.65 Å) and that of monoclinic (5.12, 5.18, and 5.28 Å)[43] and tetragonal HfO_2 (5.06 and 5.13 Å)[43] is quite similar, permitting the possibility of epitaxial growth. This finding may have severe implications about the potential use of the HfO_2/GaAs system in electronic devices.

Growth of HfO_2 films on etched GaAs surfaces.— The well-behaved growth observed for the GaAs native oxide makes the initial enhanced growth obtained for both the etched GaAs surfaces in either HF or NH_4OH even more extraordinary. For both of these surfaces, the hafnium CPC approaches that of the bulk growth after ~10 process cycles, indicating that the growth enhancement has its cause on the starting surface. These two treatments are hypothesized to produce different starting surface termination, hydroxyl termination for the NH_4OH and hydrogen termination for the HF that should affect the initial film growth. For example, on Si surfaces, termination has been shown to affect the initial film growth, resulting in an initial lower surface coverage for the Si–H surface compared to Si–OH.[19,44] Clearly, this is not the case for GaAs surfaces. For the treatment protocols used in this work, it has been shown that there is some residual arsenic and gallium oxide left on the surface.[15] If these residual oxides are in the form of oxide islands, the induced surface roughness may result in a total increase in the available surface area for film growth. However, a twofold to threefold increase in the initial hafnium CPC would imply a large degree of surface roughness, which has not been observed for similar treatments.[24] Atmospheric atomic force microscopy imaging of the surface is not very conclusive as the surface may partially reoxidize in the time it takes to complete a high resolution scan.

Conclusions

The growth and interface of ALD HfO_2 films on native oxide and pretreated GaAs surfaces have been studied with RBS, XPS, and HRTEM. The growth of the films on the native oxide surfaces is slow for the first 10–20 cycles but proceeds in a linear manner thereafter. HF- or NH_4OH-etched GaAs surfaces initially show (up to 10 cycles) a two to three times higher Hf atom coverage compared to native oxide surfaces. A gradual thinning of the surface native oxides is observed with XPS and corroborated by HRTEM data. Arsenic oxides are easier to remove, and after 100 process cycles, most of the arsenic and gallium oxides have been removed from the interface. Deposition on HF- or NH_4OH-treated surfaces show very little interface oxidation. The HRTEM data indicate that the as-deposited HfO_2 films are polycrystalline with varying grain orientations.

Acknowledgments

Acknowledgment is made to the Donors of the American Chemical Society Petroleum Research Fund and the NSF (DMR-0846445) for partial support of this research. The authors also acknowledge Karen G. Gaskell from the XPS facility of the University of Maryland for taking the data and many helpful discussions.

University of Maryland Baltimore County assisted in meeting the publication costs of this article.

References

1. R. M. C. de Almeida and I. J. R. Baumvol, *Surf. Sci. Rep.*, **49**, 1 (2003).
2. G. Wilk, R. M. Wallace, and J. M. Anthony, *J. Appl. Phys.*, **89**, 5243 (2001).
3. J. Robertson and B. Falabretti, *J. Appl. Phys.*, **100**, 014111 (2006).
4. C. X. Li, P. T. Lai, and J. P. Xu, *Microelectron. Eng.*, **84**, 2340 (2007).
5. Y. Xuan, H. C. Lin, and P. D. Ye, *IEEE Trans. Electron Devices*, **54**, 1811 (2007).
6. Y. Xuan, P. D. Ye, and T. Shen, *Appl. Phys. Lett.*, **91**, 232107 (2007).
7. S. J. Koester, E. W. Kiewra, Y. Sun, D. A. Neumayer, J. A. Ott, M. Copel, and D. K. Sadana, *Appl. Phys. Lett.*, **89**, 042104 (2006).
8. P. D. Ye, *J. Vac. Sci. Technol. A*, **26**, 697 (2008).
9. P. D. Ye, G. D. Wilk, B. Yang, J. Kwo, S. N. G. Chu, S. Nakahara, H.-J. L. Gossmann, J. P. Mannaerts, M. Hong, K. K. Ng, et al., *Appl. Phys. Lett.*, **83**, 180 (2003).
10. M. M. Frank, G. D. Wilk, D. Starodub, T. Gustafsson, E. Garfunkel, Y. J. Chabal, J. Grazul, and D. A. Muller, *Appl. Phys. Lett.*, **86**, 152904 (2005).
11. M. L. Huang, Y. C. Chang, C. H. Chang, Y. J. Lee, P. Chang, J. Kwo, T. B. Wu, and M. Hong, *Appl. Phys. Lett.*, **87**, 252104 (2005).
12. C.-H. Chang, Y.-K. Chiou, Y.-C. Chang, K.-Y. Lee, T.-D. Lin, T.-B. Wu, M. Hong, and J. Kwo, *Appl. Phys. Lett.*, **89**, 242911 (2006).
13. C. L. Hinkle, A. M. Sonnet, E. M. Vogel, S. McDonnell, G. J. Hughes, M. Milojevic, B. Lee, F. S. Aguirre-Tostado, K. J. Choi, H. C. Kim, et al., *Appl. Phys. Lett.*, **92**, 071901 (2008).
14. Y. C. Chang, M. L. Huang, K. Y. Lee, Y. J. Lee, T. D. Lin, M. Hong, J. Kwo, T. S. Lay, C. C. Liao, and K. Y. Cheng, *Appl. Phys. Lett.*, **92**, 072901 (2008).
15. J. C. Hackley, J. D. Demaree, and T. Gougousi, *Appl. Phys. Lett.*, **92**, 162902 (2008).
16. D. Shahrjerdi, D. I. Garcia-Gutierrez, E. Tutuc, and S. K. Banerjee, *Appl. Phys. Lett.*, **92**, 223501 (2008).
17. M. Milojevic, F. S. Aguirre-Tostado, C. L. Hinkle, H. C. Kim, E. M. Vogel, J. Kim, and R. M. Wallace, *Appl. Phys. Lett.*, **93**, 202902 (2008).
18. T. Gougousi and J. W. Lacis, *Thin Solid Films*, **518**, 2006–2009 (2010).
19. J. C. Hackley, T. Gougousi, and J. D. Demaree, *J. Appl. Phys.*, **102**, 034101 (2007).
20. D. M. Hausmann, E. Kim, J. Becker, and R. G. Gordon, *Chem. Mater.*, **14**, 4350 (2002).
21. H. P. Wampler, D. Y. Zemlyanov, K. Lee, D. B. Janes, and A. Ivanisevic, *Langmuir*, **24**, 3164 (2008).
22. C. C. Surdu-Bob, S. O. Saied, and J. L. Sullivan, *Appl. Surf. Sci.*, **183**, 126 (2001).
23. M. V. Lebedev, D. Ensling, R. Hunger, T. Mayer, and W. Jaegermann, *Appl. Surf. Sci.*, **229**, 226 (2004).
24. M. Rei Vilar, J. E. Beghdadi, F. Debontridder, R. Artzi, R. Naaman, A. M. Ferraria, and A. M. Botelho do Rego, *Surf. Interface Anal.*, **37**, 673 (2005).
25. L. R. Doolittle, *Nucl. Instrum. Methods Phys. Res. B*, **B15**, 227 (1986).
26. M. J. Kelly, J. H. Han, C. B. Musgrave, and G. N. Parsons, *Chem. Mater.*, **17**, 5305 (2005).
27. D. Marx, H. Asahi, X. F. Liu, M. Higashiwaki, A. B. Villaflor, K. Miki, K. Yamamoto, S. Gonda, S. Shimomura, and S. Hiyamizu, *J. Cryst. Growth*, **150**, 551 (1995).
28. S. Gonda, H. Asahi, K. Yamamoto, K. Hidaka, J. Sato, T. Tashima, and K. Asami, *Appl. Surf. Sci.*, **130–132**, 377 (1998).
29. T. J. Whitaker, T. Martin, A. D. Johnson, A. J. Pidduck, and J. P. Newey, *J. Cryst. Growth*, **164**, 125 (1996).
30. S. Salim, C. K. Lim, and K. F. Jensen, *Chem. Mater.*, **7**, 507 (1995).
31. B. Q. Shi and C. W. Tu, *J. Electron. Mater.*, **28**, 43 (1999).
32. G. Hollinger, R. Skheyta-Kabbani, and M. Gendry, *Phys. Rev. B*, **49**, 11159 (1994).
33. R. Suri, D. J. Lichtenwalner, and V. Misra, *Appl. Phys. Lett.*, **92**, 243506 (2008).
34. I. Karpov, N. Venkateswaran, G. Bratina, W. Gladfelter, A. Franciosi, and L. Sorba, *J. Vac. Sci. Technol. B*, **13**, 2041 (1995).
35. C. M. Finnie, X. Li, and P. W. Bohn, *J. Appl. Phys.*, **86**, 4997 (1999).
36. G. V. Samsonov, *The Oxide Handbook*, Plenum, New York (1973).
37. A. J. Bard, R. Parsons, and J. Jordan, *Standard Potentials in Aqueous Solutions*, Dekker, New York (1985).

38. R. D. Srivastava and M. Farber, *Chem. Rev. (Washington, D.C.)*, **78**, 627 (1978).
39. D. L. Winn, M. J. Hale, T. J. Grassman, J. Z. Sexton, and A. C. Kummel, *J. Chem. Phys.*, **127**, 134705 (2007).
40. C. L. Hinkle, M. Milojevic, B. Brennan, A. M. Sonnet, F. S. Aguirre-Tostado, G. J. Hughes, E. M. Vogel, and R. M. Wallace, *Appl. Phys. Lett.*, **94**, 162101 (2009).
41. M. J. Hale, S. I. Yi, J. Z. Sexton, A. C. Kummel, and M. Passlack, *J. Chem. Phys.*, **119**, 6719 (2003).
42. J. C. Hackley and T. Gougousi, *Thin Solid Films*, **517**, 6576 (2009).
43. U. V. Waghmare and K. M. Rabe, in *Materials Fundamentals of Gate Dielectrics*, A. A. Demkov and A. Navrotsky, Editors, p. 243, Springer, Dordrecht (2005).
44. J. C. Hackley, J. D. Demaree, and T. Gougousi, *J. Vac. Sci. Technol. A*, **26**, 1235 (2008).